Bioorganic & Medicinal Chemistry Letters xxx (xxxx) xxx–xxx

Contents lists available at ScienceDirect

Bioorganic & Medicinal Chemistry Letters

journal homepage: www.elsevier.com/locate/bmcl

Dual inhibition of Kif15 by oxindole and quinazolinedione chemical probes

Megan E. Dumas[a], Geng-Yuan Chen[b,1], Nicole D. Kendrick[a], George Xu[c], Scott A. Larsen[d], Somnath Jana[e], Alex G. Waterson[e,f,g], Joshua A. Bauer[h], William Hancock[b], Gary A. Sulikowski[f], Ryoma Ohi[c,i,*]

[a] Department of Cell and Developmental Biology, Vanderbilt University, Nashville, TN 37232, United States
[b] Department of Biomedical Engineering, Pennsylvania State University, State College, PA, United States
[c] Department of Cell and Developmental Biology, University of Michigan Medical School, Ann Arbor, MI 48109, United States
[d] Department of Medicinal Chemistry, University of Michigan, Ann Arbor, MI 48109, United States
[e] Vanderbilt Institute of Chemical Biology, Nashville, TN 37232, United States
[f] Department of Chemistry, Vanderbilt University, Nashville, TN 37232, United States
[g] Department of Pharmacology, Vanderbilt University, Nashville, TN 37232, United States
[h] Department of Biochemistry, Vanderbilt University, Nashville, TN 37232, United States
[i] Life Sciences Institute, University of Michigan, Ann Arbor, MI 48109, United States

ARTICLE INFO

Keywords:
Kinesin
Mitosis
Oxindole
Kif15
Eg5

ABSTRACT

The mitotic spindle is a microtubule-based machine that segregates a replicated set of chromosomes during cell division. Many cancer drugs alter or disrupt the microtubules that form the mitotic spindle. Microtubule-dependent molecular motors that function during mitosis are logical alternative mitotic targets for drug development. Eg5 (Kinesin-5) and Kif15 (Kinesin-12), in particular, are an attractive pair of motor proteins, as they work in concert to drive centrosome separation and promote spindle bipolarity. Furthermore, we hypothesize that the clinical failure of Eg5 inhibitors may be (in part) due to compensation by Kif15. In order to test this idea, we screened a small library of kinase inhibitors and identified GW108X, an oxindole that inhibits Kif15 *in vitro*. We show that GW108X has a distinct mechanism of action compared with a commercially available Kif15 inhibitor, Kif15-IN-1 and may serve as a lead with which to further develop Kif15 inhibitors as clinically relevant agents.

Cells sustain life by dividing. The division process, which includes mitosis and cytokinesis, is a logical target for cancer therapy, particularly in cancer cells that exhibit growth rates higher than most normal tissues. Chemotherapeutics that act by derailing cell division are termed "anti-mitotics".[1] The archetypal class of anti-mitotics target microtubules (MTs), which are the major component of the mitotic spindle, the apparatus that segregates chromosomes during mitosis. Paclitaxel, the best known MT toxin, is a blockbuster cancer drug and is commonly used to treat a wide range of tumors.[2] Despite the success of MT-targeting agents, they commonly cause side effects (*e.g.*, neutropenia, peripheral neuropathy), reflecting the widespread importance of MTs in cell function.[3]

To minimize collateral damage, next generation anti-mitotics target proteins with mitosis-specific functions, such as kinases (*e.g.*, Aurora and Polo kinases) and MT-dependent motor proteins (*i.e.*, dynein and mitotic kinesins) involved in the assembly and remodeling of the mitotic spindle.[4] The first clinically targeted kinesin was Eg5, a kinesin-5 family member that slides pairs of anti-parallel MTs apart to drive centrosome separation, which is the key step in the establishment of spindle bipolarity. When Eg5 is inhibited, the spindle fails to bipolarize and instead forms a monopolar spindle.[5] A multitude of kinesin-5 inhibitors (K5I) that act *via* distinct mechanisms have been developed and characterized.[6] All clinically relevant K5Is are allosteric inhibitors that bind near the Loop5 region of the Eg5 motor and decrease its affinity for MTs.[7] While K5Is show robust anti-proliferative activity in cell and mouse tumor models, they have largely failed in the clinic.[6] The underlying reason(s) for K5I failure remain unclear, but one hypothesis is that there are cellular mechanisms that can compensate for a loss of Eg5 activity.

Consistent with the idea that an auxiliary spindle assembly mechanism can substitute for the Eg5-driven pathway, a second mitotic kinesin, Kif15, can promote spindle assembly in the absence of Eg5

* Corresponding author at: Department of Cell and Developmental Biology, University of Michigan Medical School, Ann Arbor, MI 48109, United States.
E-mail address: oryoma@umich.edu (R. Ohi).
[1] Current address: Department of Biology, University of Pennsylvania, Philadelphia, PA 19104.

https://doi.org/10.1016/j.bmcl.2018.12.008
Received 19 October 2018; Received in revised form 30 November 2018; Accepted 4 December 2018

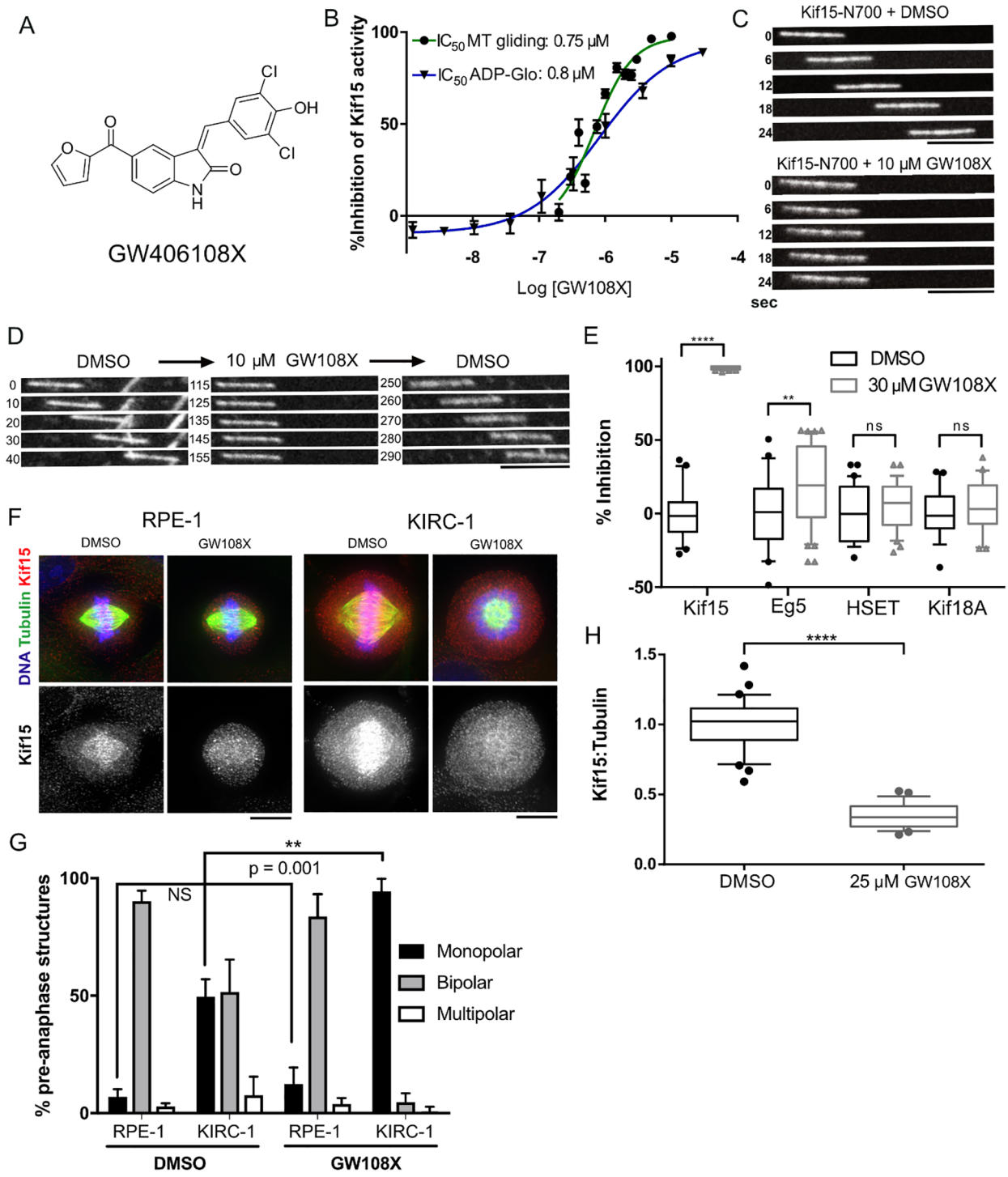

Fig. 1. GW406108X (GW108X) inhibits and displays preference for Kif15. (A) Structure of GW108X. (B) Concentration response curves (CRC) generated from the ATPase (blue line) and MT gliding (green line) assay. CRC from the ATPase assay was developed from 10 concentrations from 30 to 0.001 μM. Each concentration was repeated in triplicate. CRC from the MT gliding assay was developed from 12 concentrations from 10 to 0.2 μM. Error bars show SEM. (C) Representative montage of a fluorescent MT in a gliding assay with Kif15-N700 with DMSO (top) or 10 μM of GW108X (bottom). Numbers indicate time in seconds after initial frame. Scale bar, 5 μm. (D) Representative montage of fluorescent MTs from the double wash out experiment. Numbers indicate time in seconds after initial frame, which are not the same MT for each condition. Scale bar, 5 μm. (E) Percent inhibition of indicated mitotic motors treated with 30 μM of GW108X. n > 20 for all conditions, $^{****}p < 0.0001$, $^{**}p = 0.0074$. (F) Max intensity z-projections of *TP53*$^{-/-}$ RPE-1 (left) and KIRC-1 (right) cells treated with DMSO or 25 μM GW108X for 24 h and stained with antibodies targeting Kif15 (grayscale and red), tubulin (green) and DNA (blue). Lookup tables (LUTs) for grayscale, red, and green channel are scaled identically. Scale bar, 10 μm. (G) Quantitation of % of pre-anaphase structures in *TP53*$^{-/-}$ RPE-1 and KIRC-1 cells treated with DMSO or 25 μM GW108X for 24 h. Each condition was tested in triplicate and n ≥ 100 cells per replicate were counted. Errors bars show SD. (H) Quantitation of Kif15 on metaphase MTs in *TP53*$^{-/-}$ RPE-1 cells treated with DMSO or 25 μM GW108X. Shown are ratios of Kif15 fluorescence intensities to tubulin intensities. Box-and-whisker plots describe the median value as well as the 10th, 25th, 75th and 90th percentiles. $^{****}p < 0.0001$. n ≥ 25 cells from triplicate experiments.

activity.[8–11] The importance of Kif15 in K5I-resistance is highlighted by our recent discovery that deletion of *KIF15* prevents the emergence of K5I resistance in cultured cells. This finding raises the possibility that therapies targeting spindle assembly will not be efficacious unless Kif15 inhibitors are also included.[10]

We set out to identify chemical scaffolds that target Kif15 as a starting point for tool compound development and drug design. We screened the GlaxoSmithKline Published Kinase Inhibitor set (GSK PKIS) and identified two oxindole compounds that inhibit Kif15 ATPase activity. GW406108X (hereafter GW108X) and GW305074X (**2**) inhibited Kif15-N420 ATPase activity by 76 ± 3.6% and 90 ± 5.3%, respectively (Figs. 1A, S1B, and S2A). Both compounds contain an oxindole core and a halogenated phenol ring on the right-hand side of the molecule. They differ most at the 5-position of the oxindole, with GW108X being an acylfuran and **2** being an iodide. Oxindoles are a class of privileged scaffolds that have been frequently used as starting points for kinase inhibitors, but this scaffold has previously been used to generate a myosin V inhibitor.[12] GW108X and **2** were first described as potent c-Raf1 inhibitors and have since been extensively characterized by GSK, with GW108X reported as being a promiscuous kinase and GPCR inhibitor.[13–16]

Concentration response analysis for GW108X and **2** was performed using the ATPase assay, generating IC_{50} values of 0.82 μM for GW108X and 2.5 μM for **2** (Figs. 1B (blue curve) and S2B). We decided to pursue GW108X for further analysis because of its sub-micromolar IC_{50}. To further characterize the ability of GW108X to inhibit Kif15, we used the MT-gliding assay. For this, we used Kif15-N700, a longer construct that robustly glides MTs (see Materials and Methods).[17] The inhibitory activity of GW108X against Kif15 was scored by calculating the velocity of MT gliding over a range of inhibitor concentrations to generate a concentration response curve. The IC_{50} was 734 nM, similar to that calculated using the ATPase assay (Fig. 1B (green curve) and C).

We next used the MT gliding assay to test whether the inhibition of Kif15 by GW108X is reversible. We initiated MT gliding by Kif15 in the presence of DMSO, and then introduced 10 μM of GW108X. Treatment for 1 min was sufficient to eliminate MT gliding. GW108X was then washed out, and the chamber was imaged for another minute. After wash out of GW108X, MTs resumed gliding again, revealing that GW108X inhibits Kif15 in a reversible manner (Fig. 1D, Supporting Video 2). MT gliding was unaffected when only DMSO was washed in (Fig. S2C). We then tested the ability of GW108X to inhibit Eg5, HSET, and Kif18A, three additional mitotic motors that differ in both structure and function.[18–20] Despite promiscuity as a kinase inhibitor, GW108X displayed a preference for Kif15 over the other mitotic motors, with 30 μM of GW108X inhibiting Kif15 MT gliding by 98.9% ± 0.2% while only inhibiting Eg5 by 19.8% ± 4.3%, HSET by 5.3% ± 2.9% and Kif18A by 4.9% ± 3.9 (mean ± SEM, Fig. 1E). Taken together, these assays show that GW108X has the ability to reversibly inhibit Kif15 and suggests that the compound may exploit a Kif15-specific binding site for inhibition.

To determine if GW108X affects Kif15 activity in cells, we first analyzed its effects on Kif15 localization and activity in *TP53*$^{-/-}$ RPE-1 cells.[21] In RPE-1 cells treated with 25 μM GW108X, 84% of pre-anaphase microtubule arrays were bipolar (n = 470), similar to cells treated with DMSO (90% bipolar, n = 490), which is consistent with previous work showing that Kif15 is not normally required for spindle assembly (Fig. 1G).[11,22] However, 25 μM of GW108X led to a 3-fold decrease of spindle-bound Kif15 levels compared to DMSO, as assessed by quantitative immunofluorescence microscopy (Fig. 1F and H). Decrease in Kif15 levels on the spindle corresponds to a ~60% decrease in Kif15 protein levels in RPE-1 cells treated with 25 μM GW108X, suggesting that GW108X treatment of cells leads to Kif15 degradation (Fig. S3A and B). Despite a decrease of Kif15 in RPE-1 cells treated with 25 μM GW108X, spindle lengths were unaffected (Fig. S3C).

To determine if GW108X inhibits the spindle assembly function of Kif15, we tested whether GW108X blocks spindle assembly in an RPE-1 cell line adapted to survive in the presence of the kinesin-5 inhibitor STLC. Cancer cells can acquire resistance to K5Is, and these K5I-resistant cell lines (KIRCs) rely on Kif15 to build a bipolar spindle.[8–11] We generated the KIRC-1 cell line as a clone of *TP53*$^{-/-}$ RPE-1 cells that adapted to the presence of 10 μM STLC (see Materials and Methods). Without further perturbation, KIRC-1 cells exhibit ~50–60% monopolar spindles, consistent with previously published K5I-resistant lines (Fig 1F and G).[11] Confirming that Kif15 is essential to complete cell division when Eg5 is inhibited, depletion of Kif15 from KIRC-1 cells by RNAi blocked bipolar spindle assembly; 99% of Kif15-depleted KIRC-1 cells contained monopolar spindles, compared to 65% in control siRNA-transfected cells (Fig. S3D and E). To test the effects of GW108X, we scored monopolarity in KIRC-1 cells treated with 25 μM of GW108X (in the presence of 10 μM STLC), and found that the compound increased the percent of monopolar spindles in KIRC-1 cells from 49 ± 4% to 95 ± 3% (Fig. 1F and G). The ability of GW108X to block spindle assembly in KIRC-1 cells was dose-dependent (Fig. S3F).

In KIRC-1 cells, Kif15 is required for spindle bipolarity (Fig. S3D), but we cannot exclude the possibility that the increase of monopolar spindles in the presence of GW108X is not due to mechanisms beyond Kif15 inhibition. Since GW108X is a broad-spectrum kinase inhibitor, it is possible that a block in spindle assembly is partly due to co-inhibition of a mitotic kinase(s). Importantly, such kinase inhibitor activity is tolerated in RPE-1 cells, as spindle assembly is not prevented in the parental cell line. In HeLa K5I-resistant cell lines, monopolar spindles can arise from the combined inhibition of Eg5 and Aurora A Kinase (AURKA).[8] Furthermore, phosphorylation of Kif15 by AURKA is required to target Kif15 to the spindle.[23] While biochemical analysis revealed that GW108X inhibits AURKA 67% at 1 μM, it is unknown if GW108X effectively inhibits AURKA in cells.[13]

To probe the relationship between structure and Kif15 inhibition activity of GW108X, we created a small library of derivatives with modifications to both the furan and the phenol. The compounds were prepared according to Scheme 1 (Fig. 2). We first explored conservative changes around the hit compound. The requisite intermediate **II** was synthesized from a Friedel-Crafts reaction from oxindole **I**. Condensation with various aromatic aldehydes gave the GW108X-inspired analogs **III**. We also contemplated changes to the oxindole 5-position substituent. Analogs **V**, with a furan or other aromatic ring directly attached to the oxindole, were generated using palladium-mediated Suzuki coupling reactions from readily accessible bromides **IV**. Similarly, acids **VI** could be derivatized to corresponding amides **VIII** using HATU-based amide coupling conditions.

To compare the activity of the GW108X derivatives, we tested their ability to inhibit Kif15 MT-gliding at 750 nM, roughly the IC_{50} of GW108X (Fig. 3). GW108X contains halogens in the ortho positions of the phenol, which may provide opportunities for the formation of both

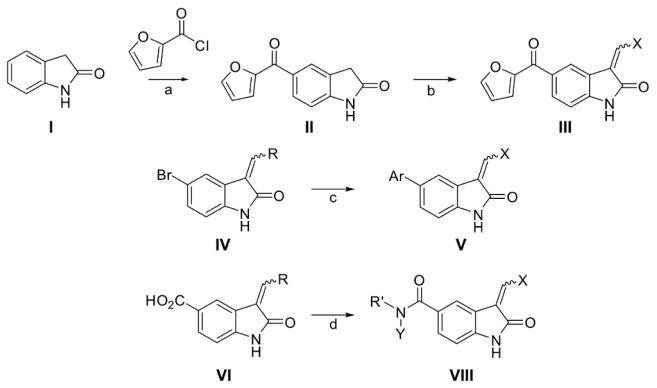

Fig. 2. Scheme 1. Reagents and conditions: a. $AlCl_3$, DCE. 0 °C, 65% b. RCHO, piperidine, EtOH, 80 °C, 40–70% c. $ArB(OH)_2$, $Pd(PH_3)_4$, Na_2CO_3, 2:1 dioxane/water, 110 °C, 20–79% d. amine, HATU, DIPEA, DMF, 57–64%.

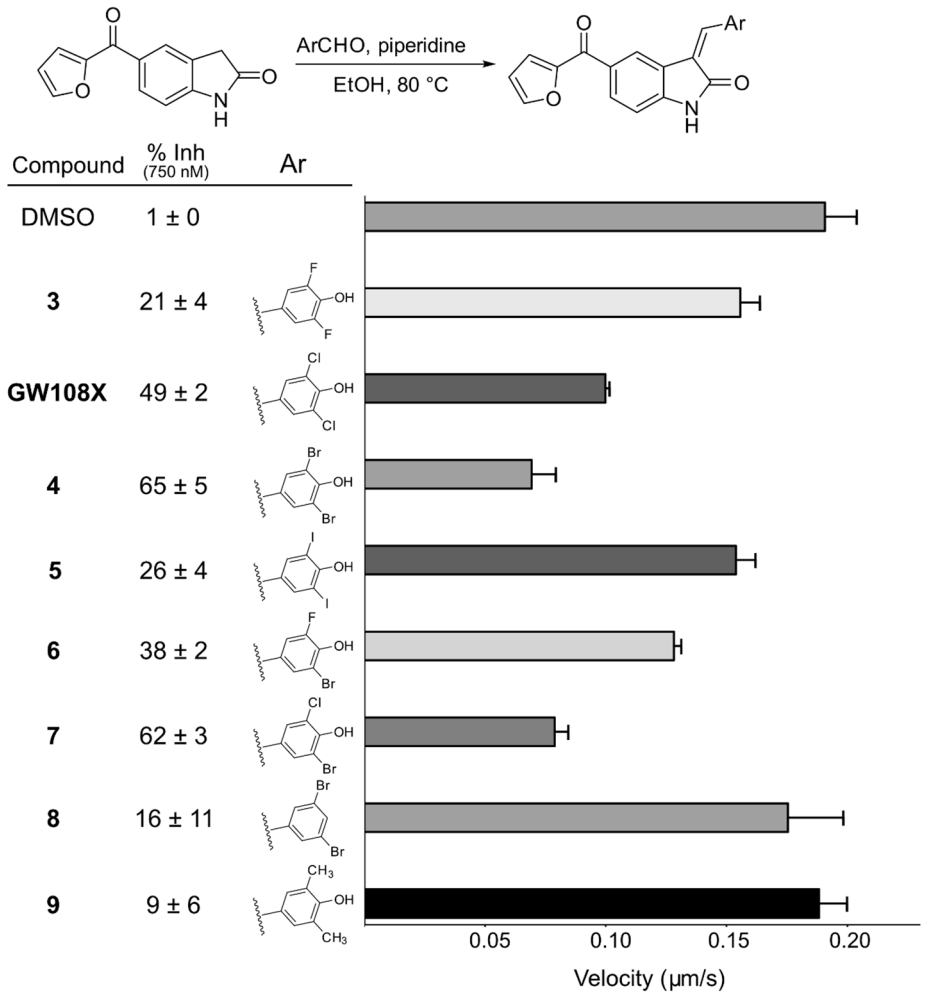

Fig. 3. Structure-activity relationship (SAR) analysis of GW108X derivatives. Representative compounds from SAR library of phenol derivatives tested at 750 nM. Data is the average microtubule gliding velocity of Kif15-N700 with each compound. Every compound was tested in triplicate with n ≥ 30 measurements for each replicate, except **8** and **5**, which were performed in duplicate. Error bars show SEM. See Table S1 for complete list of SAR compounds.

hydrogen and halogen bonds with biomolecules. Compounds **3** and **4**, with different halogens in the meta position, displayed, together with GW108X, a structure activity relationship (SAR) that correlated with halogen size. The Kif15 inhibition activity of the compound improved as the halogen size increased from fluorine to bromine, with **4** inhibiting MT gliding by 65%. Interestingly, compounds that contain two different halogens (**6** and **7**) showed intermediary inhibition also in line with respective halogen size. The larger iodines of **5**, however, were not as well tolerated, and none of the compounds showed percent inhibition significantly different than that of GW108X. Unfortunately, more aggressive changes in the aromatic ring substitutions served only to demonstrate the importance of the hydroxyl and halogens for robust inhibition of Kif15 (see also Table S1 for additional SAR). For example, removal (**8**) or substitution (**10**, Table S1) of the phenolic hydroxyl abolished activity. Furthermore, both halogen substituents appear to be required, as compounds with the halogens replaced with methyl groups (**9**) were reduced in activity. We found that the 5-position of the oxindole core was intolerant of changes, as these compounds did not robustly inhibit Kif15 MT-gliding (Table S1).

A recently described inhibitor, Kif15-IN-1, was shown to inhibit Kif15 as well as synergize with Eg5 inhibitors in both MT gliding and cell viability assays.[24] Kif15-IN-1 is a quinazolinedione, reported to have an IC_{50} of 1.72 μM in the gliding assay (Fig. 4A). Since Kif15-IN-1 recently became commercially available, we compared its activity to that of GW108X and characterized its effect on Kif15 in cells. First, we repeated MT gliding assays using the reported IC_{50} of 1.72 μM and found that this concentration abolishes Kif15-driven MT gliding (Fig. S4A). Concentration response analysis using the MT gliding assay revealed that the IC_{50} was 203 nM, significantly lower than the previous study (Fig. 4B).[24] Similar to GW108X, Kif15-IN-1 was reversible in the MT gliding assay (Fig. 4C, Supporting Video 3).

We next tested the effect of Kif15-IN-1 on Kif15 localization in RPE-1 cells by treating them with 25 μM Kif15-IN-1. Unlike GW108X, Kif15-IN-1 did not reduce spindle-bound levels of Kif15 and only decreased Kif15 protein in whole cell lysates by 15% (Fig. 4D, E, and S4B and C). Nevertheless, spindles were shorter in RPE-1 cells treated with 25 μM Kif15-IN-1 (9.9 μm ± 0.3 μm) compared to DMSO (11.4 μm ± 0.2 μm), a phenotype consistent with knock-down of Kif15 (Fig. S4D).[11,22,25] Similar to GW108X, 25 μM Kif15-IN-1 had no effect on spindle bipolarity of RPE-1 cells (96% of bipolar (n = 196) in Kif15-IN-1-treated cells, 94% bipolar in DMSO-treated cells (n = 303)). In KIRC-1 cells treated with 25 μM Kif15-IN-1, the percentage of monopolar pre-anaphase microtubule arrays increased from 43% in DMSO (n = 260) to 84% (n = 269, Fig. 4F), similar to the increase observed with GW108X.

In principle, GW108X and Kif15-IN-1 could inhibit the MT-stimulated ATPase and MT gliding activity of Kif15 either by inhibiting ATP binding or by inhibiting MT binding by the motor. To distinguish between these possibilities, we first measured the MT-stimulated ATPase activity of Kif15-N700 at varying concentrations of ATP or MTs in the presence of GW108X. When varying the concentration of a substrate, a competitive inhibitor will change the K_M while V_{max} remains

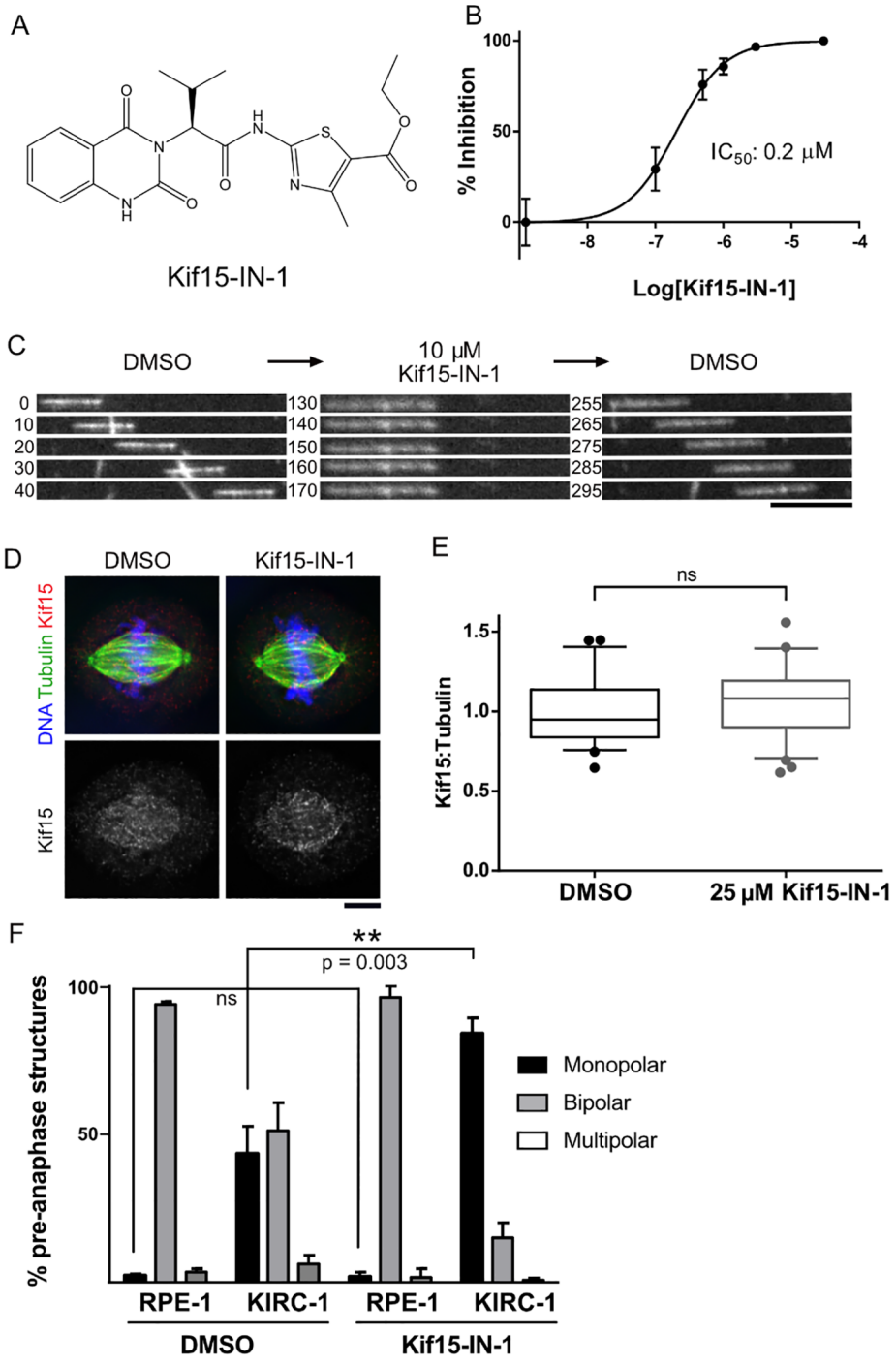

Fig. 4. Kif15-IN-1 is a sub-micromolar inhibitor of Kif15. (A) Structure of Kif15-IN-1. (B) Concentration response curve using the MT-gliding assay, developed from 5 concentrations of Kif15-IN-1, ranging from 30 to 0.1 µM. Error bars show SD. (C) Representative montage of fluorescent MTs from the double wash out experiment. Each vertical frame represents 10 s. Scale bar, 5 µm. (D) Representative single optical sections of RPE-1 cells treated with DMSO or 25 µM Kif15-IN-1 for 24 h and stained for antibodies targeting Kif15 (grayscale and red), tubulin (green) and DNA (blue). LUTs for grayscale, red and green channels are scaled identically. Scale bar, 5 µM. (E) Quantitation of RPE-1 cells treated with DMSO or 25 µM Kif15-IN-1 for 24 h. Shown are ratios of Kif15 fluorescence intensities to tubulin intensities. Box-and-whisker plots describe the median value as well as the 10th, 25th, 75th and 90th percentiles. n = 30 cells from triplicate experiments. (F) Quantitation of the % pre-anaphase structures in RPE-1 cells treated with DMSO or 25 µM Kif15-IN-1 for 24 h. Each condition was tested in triplicate and graph displays average percent from each triplicate. Errors bars show SD.

unchanged, whereas a non-competitive inhibitor will change the V_{max} with no change in the K_M. When varying ATP concentrations in the presence of GW108X at a high MT concentration, there was no change in the measured K_M^{ATP} and a decrease in the V_{max}, indicating that GW108X is not competing with ATP binding (Fig. 5A). In contrast, when the MT concentration was varied in the presence of saturating ATP, an increase in the K_M^{MT} was observed, suggesting that GW108X interferes with Kif15's MT binding ability (Fig. 5B). This result is consistent with the observed decrease of Kif15 on the spindle (Fig. 1H).

In contrast to GW108X, an increase in K_M^{ATP} was observed when the ATP concentration was varied in the presence of Kif15-IN-1, indicating that instead of competing with MT binding, Kif15-IN-1 competes with ATP binding (Fig. 5C). Since GW108X and Kif15-IN-1 display different modes of inhibition, it is unlikely that they share the same binding site within the motor and instead each offer novel chemical space for Kif15 inhibition.

This distinction in biochemical mechanism is important for two reasons. If Kif15 contains two proximal inhibitor binding sites, it may be possible to link compounds that target the two sites, creating a larger molecule with the potential to occupy both sites. Conjugation of two chemotypes might improve specificity and affinity of the inhibitor. Secondly, dual-targeting of Kif15 with GW108X and Kif15-IN-1 should decrease the possibility that *KIF15* mutations could bypass drug mechanism.[26]

Mitotic kinesin inhibitors are routinely used in cell biology laboratories and allow researchers to specifically modulate a motors activity to give a predicted perturbation of MT or spindle dynamics. For example, both ATP competitive and allosteric inhibitors of the mitotic

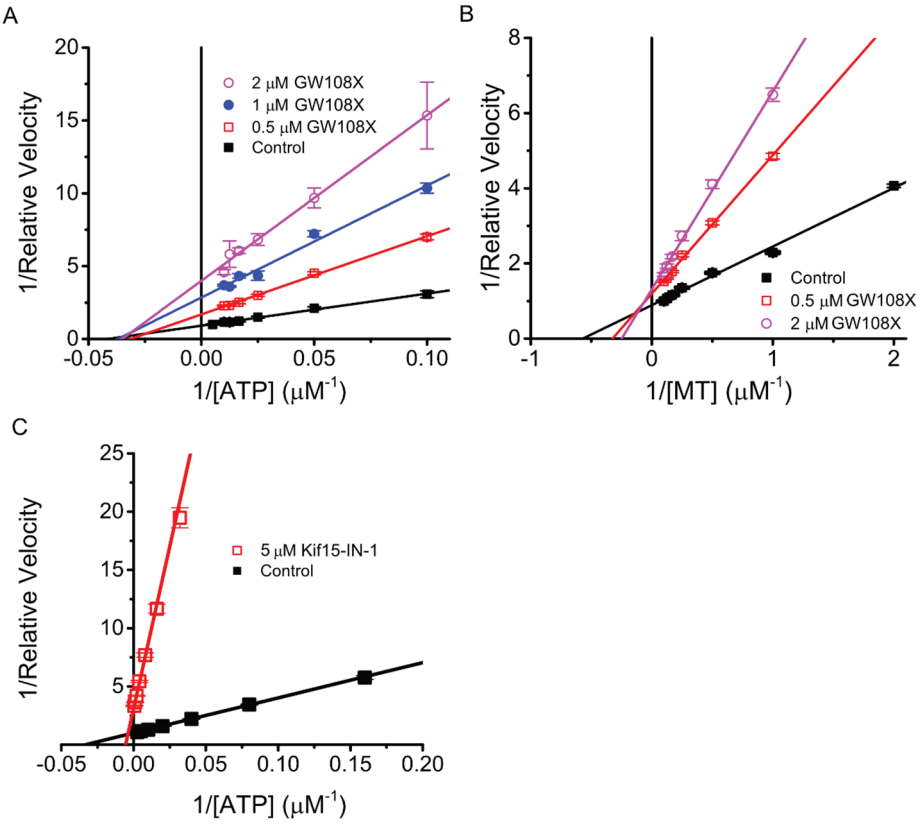

Fig. 5. Kif15-IN-1 is a competitive ATP inhibitor and GW108X is a non-competitive ATP inhibitor. (A) Double reciprocal Lineweaver-Burk plot of ATP titration at 0.5, 1 and 2 μM GW108X. (B) Double reciprocal Lineweaver-Burk plot of MT titration at 0.5 and 2 μM GW108X. (C) Double reciprocal Lineweaver-Burk plot of ATP titration using 5 μM Kif15-IN-1. Each reaction in A–C was performed in triplicate. All error bars show SEM.

motors Eg5 and CENP-E have been extensively characterized both *in vitro* and in clinical trials.[27–29] Most recently, functionally distinct K5Is were shown to have differential effects on both MT dynamics *in vitro* and spindle stability in RPE-1 cells.[30] While the canonical non-competitive loop-5 targeting K5Is result in the classic monopolar spindle phenotype, the ATP competitive inhibitor BRD9876 stabilizes MTs *in vitro* and does not cause spindle collapse. Small molecule inhibitors that can modulate Kif15's mechanochemical cycle in different ways will also be powerful tools for mitosis research. In the case of Kif15, its mitotic function under normal conditions is not well understood. Kif15 localizes to kinetochore-MTs, regulating the stability and length of these bundles.[11] When over-expressed, as in K5I-resistant cells, Kif15 relocalizes to non-KMTs and provides outward forces required for centrosome separation. Small molecules that can acutely inhibit Kif15 in these different cellular contexts through different mechanisms are likely to reveal new properties and functions of Kif15 during mitosis.

Our studies with GW108X and Kif15-IN-1 show that both compounds are useful launch points in the generation of Kif15-targeting drugs. Given that cultured cells **must** express *KIF15* in order to acquire K5I resistance[10] and that K5Is synergize with Kif15-IN-1 to decrease in cell viability[24], there is clear rationale to pursue Kif15-targeting drugs for use in combination with K5Is as a chemotherapeutic strategy.

Acknowledgments

We thank members of the R. Ohi, M. Zanic and M. Lang labs for insightful discussions and Bryan Tsou (Memorial Sloan Ketterling Cancer Center) for the RPE-1 *TP53*$^{-/-}$ cell line. We acknowledge the Vanderbilt Institute of Chemical Biology chemical synthesis core and the Vanderbilt High Throughput Screening facility for technical support and useful discussions. This work was supported by National Institutes of Health grants R01GM086610 to R. Ohi and R50 CA211206 to J.B. R. Ohi was also supported by a Scholar Career Development Award from the Leukemia and Lymphoma Society. We thank GlaxoSmithKline LCC for providing the kinase inhibitor library PKIS, https://www.sgc-unc.org/kinase-chemogenomics/.

Appendix A. Supplementary data

Supplementary data to this article can be found online at https://doi.org/10.1016/j.bmcl.2018.12.008.

References

1. van Vuuren RJ, Visagie MH, Theron AE, Joubert AM. Antimitotic drugs in the treatment of cancer. *Cancer Chemother Pharmacol.* 2015;76(6):1101–1112.
2. Huang TC, Campbell TC. Comparison of weekly versus every 3 weeks paclitaxel in the treatment of advanced solid tumors: a meta-analysis. *Cancer Treat Rev.* 2012;38(6):613–617.
3. Ferrier J, Pereira V, Busserolles J, Authier N, Balayssac D. Emerging trends in understanding chemotherapy-induced peripheral neuropathy. *Curr Pain Headache Rep.* 2013;17(10):364.
4. Dominguez-Brauer C, Thu KL, Mason JM, Blaser H, Bray MR, Mak TW. Targeting mitosis in cancer: emerging strategies. *Mol Cell.* 2015;60(4):524–536.
5. Mayer TU, Kapoor TM, Haggarty SJ, King RW, Schreiber SL, Mitchison TJ. Small molecule inhibitor of mitotic spindle bipolarity identified in a phenotype-based screen. *Science.* 1999;286(5441):971–974.
6. Rath O, Kozielski F. Kinesins and cancer. *Nat Rev Cancer.* 2012;12(8):527–539.
7. Waitzman JS, Larson AG, Cochran JC, et al. The loop 5 element structurally and kinetically coordinates dimers of the human kinesin-5, Eg5. *Biophys J.* 2011;101(11):2760–2769.
8. Ma HT, Erdal S, Huang S, Poon RY. Synergism between inhibitors of Aurora A and KIF11 overcomes KIF15-dependent drug resistance. *Mol Oncol.* 2014;8(8):1404–1418.
9. Raaijmakers JA, van Heesbeen RG, Meaders JL, et al. Nuclear envelope-associated dynein drives prophase centrosome separation and enables Eg5-independent bipolar spindle formation. *EMBO J.* 2012.
10. Sturgill EG, Norris SR, Guo Y, Ohi R. Kinesin-5 inhibitor resistance is driven by kinesin-12. *J Cell Biol.* 2016;213(2):213–227.
11. Sturgill EG, Ohi R. Kinesin-12 differentially affects spindle assembly depending on its microtubule substrate. *Curr Biol.* 2013;23(14):1280–1290.
12. Islam K, Chin HF, Olivares AO, Saunders LP, De La Cruz EM, Kapoor TM. A myosin V inhibitor based on privileged chemical scaffolds. *Angew Chem Int Ed Engl.* 2010;49(45):8484–8488.
13. Elkins JM, Fedele V, Szklarz M, et al. Comprehensive characterization of the published kinase inhibitor set. *Nat Biotechnol.* 2016;34(1):95–103.

14. Lackey K, Cory M, Davis R, et al. The discovery of potent cRaf1 kinase inhibitors. *Bioorg Med Chem Lett.* 2000;10(3):223–226.
15. Richters A, Basu D, Engel J, et al. Identification and further development of potent TBK1 inhibitors. *ACS Chem Biol.* 2015;10(1):289–298.
16. Lai JYQ, Cox PJ, Patel R, et al. Potent small molecule inhibitors of spleen tyrosine kinase (Syk). *Bioorg Med Chem Lett.* 2003;13(18):3111–3114.
17. Sturgill EG, Das DK, Takizawa Y, et al. Kinesin-12 Kif15 targets kinetochore fibers through an intrinsic two-step mechanism. *Curr Biol.* 2014;24(19):2307–2313.
18. Mountain V, Simerly C, Howard L, Ando A, Schatten G, Compton DA. The kinesin-related protein, HSET, opposes the activity of Eg5 and cross-links microtubules in the mammalian mitotic spindle. *J Cell Biol.* 1999;147(2):351–366.
19. Stumpff J, von Dassow G, Wagenbach M, Asbury C, Wordeman L. The kinesin-8 motor Kif18A suppresses kinetochore movements to control mitotic chromosome alignment. *Dev Cell.* 2008;14(2):252–262.
20. Turner J, Anderson R, Guo J, Beraud C, Fletterick R, Sakowicz R. Crystal structure of the mitotic spindle kinesin Eg5 reveals a novel conformation of the neck-linker. *J Biol Chem.* 2001;276(27):25496–25502.
21. Izquierdo D, Wang WJ, Uryu K, Tsou MF. Stabilization of cartwheel-less centrioles for duplication requires CEP295-mediated centriole-to-centrosome conversion. *Cell Rep.* 2014;8(4):957–965.
22. Vanneste D, Takagi M, Imamoto N, Vernos I. The role of Hklp2 in the stabilization and maintenance of spindle bipolarity. *Curr Biol.* 2009;19(20):1712–1717.
23. van Heesbeen R, Raaijmakers JA, Tanenbaum ME, et al. Aurora A, MCAK, and Kif18b promote Eg5-independent spindle formation. *Chromosoma.* 2017;126(4):473–486.
24. Milic B, Chakraborty A, Han K, Bassik MC, Block SM. KIF15 nanomechanics and kinesin inhibitors, with implications for cancer chemotherapeutics. *PNAS.* 2018;115(20):E4613–E4622.
25. Tanenbaum ME, Macurek L, Janssen A, Geers EF, Alvarez-Fernandez M, Medema RH. Kif15 cooperates with eg5 to promote bipolar spindle assembly. *Curr Biol.* 2009;19(20):1703–1711.
26. Schmitt MW, Loeb LA, Salk JJ. The influence of subclonal resistance mutations on targeted cancer therapy. *Nat Rev Clin Oncol.* 2016;13(6):335–347.
27. Kantarjian HM, Padmanabhan S, Stock W, et al. Phase I/II multicenter study to assess the safety, tolerability, pharmacokinetics and pharmacodynamics of AZD4877 in patients with refractory acute myeloid leukemia. *Invest New Drugs.* 2012;30(3):1107–1115.
28. Rickert KW, Schaber M, Torrent M, et al. Discovery and biochemical characterization of selective ATP competitive inhibitors of the human mitotic kinesin KSP. *Arch Biochem Biophys.* 2008;469(2):220–231.
29. Wood KW, Lad L, Luo L, et al. Antitumor activity of an allosteric inhibitor of centromere-associated protein-E. *PNAS.* 2010;107(13):5839–5844.
30. Chen GY, Kang YJ, Gayek AS, et al. Eg5 inhibitors have contrasting effects on microtubule stability and metaphase spindle integrity. *ACS Chem Biol.* 2017;12(4):1038–1046.